Thermoelectric power of graphite intercalation compounds

Ko Sugihara*

Center for Materials Science and Engineering, Massachusetts Institute of Technology, Cambridge, Massachusetts 02139

(Received 4 February 1983)

A model for the temperature variations of the thermoelectric power (TEP) of acceptor graphite intercalation compounds (GIC's) is presented. At low temperatures, the TEP in GIC's increases monotonically with T, then levels off above ~ 200 K in striking contrast to that of pristine graphite. The diffusion contribution to the TEP is proportional to T and its magnitude is small as compared with that of the observed data. This observed behavior is attributed to the phonon drag effect. In the temperature region where the TEP is weakly temperature dependent, phonon relaxation is mainly controlled by the Rayleigh scattering due to point defects. The resultant TEP, which is composed of the phonon drag and diffusion terms, leads to a nearly T-independent value. Since the cross-sectional diameter of the Fermi surface in GIC's is larger than that of pristine graphite, the relaxation rate of the Rayleigh scattering, which is given by $1/t_l(q)=fq^3$, becomes very large at high temperatures $(T > 100$ K). At low temperatures, where the boundary scattering plays a dominant role, the TEP is proportional to T^3. Detailed calculations are carried out by solving the phonon-carrier-coupled Boltzmann equation.

I. INTRODUCTION

Studies of the transport properties of graphite intercalation compounds (GIC's) have attracted a good deal of attention from many investigators.[1] Among the various techniques, the measurements of the thermoelectric power (TEP) provide useful information on the Fermi energy, energy dependence of the carrier-relaxation time, strength of the electron-phonon coupling, and the phonon-relaxation processes. Recently, the thermal conductivity, TEP (a-axis and c-axis values), and c-axis resistivity of $FeCl_3$-intercalated graphite and a stage-5 potassium GIC have been measured.[2-5]

Detailed measurements on the TEP and thermal conductivity of $SbCl_5$-intercalated graphite spanning stages 2—10 have been carried out by Elzinga et al.,[6] Figs. 1 and 2 indicate a typical feature of the TEP in the acceptor compounds.[2,6] These curves indicate that the TEP in
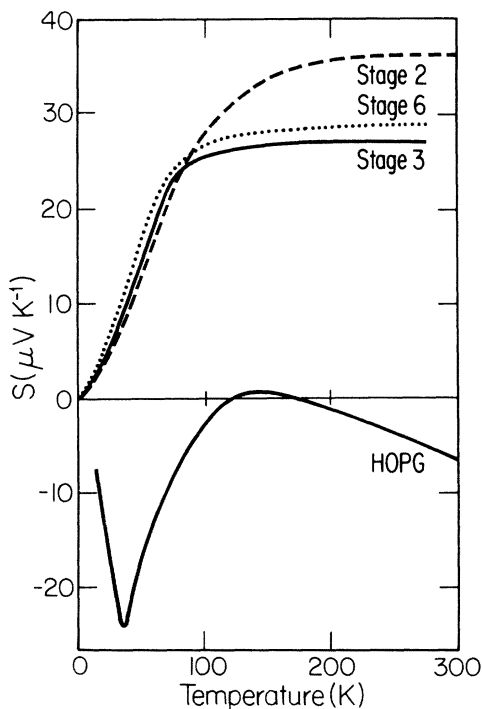

FIG. 1. Temperature variation of the TEP of the three $FeCl_3$-intercalated graphite compounds compared to that of pristine graphite (Refs. 2 and 3).
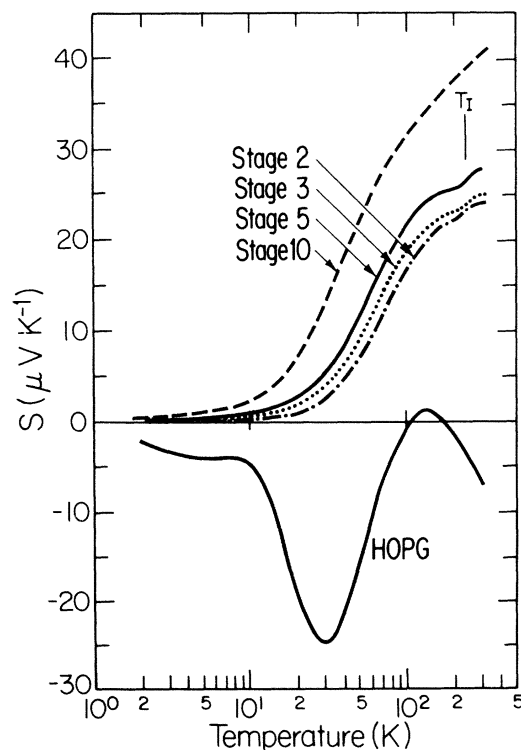

FIG. 2. Temperature dependence of the TEP of $SbCl_5$-intercalated graphite compounds. T_I marks the temperature of the commensurate-incommensurate transition (Ref. 6).

GIC's exhibits a different T dependence from that of a pristine graphite and that it is nearly stage independent except for a high-stage compound.[2,6]

Highly crystalline graphite exhibits a large negative dip of the TEP around 35 K,[2,6,7] and this anomaly was ascribed to the phonon drag effect.[7-10] In this paper it is shown that T dependence of the TEP in GIC's is also explainable in terms of the phonon drag effect. Since the carrier density in GIC's is 1 or 2 orders of magnitude larger than that of pristine graphite,[1] the cross-sectional diameter of the Fermi surface of GIC's is much larger. This affects the phonon drag TEP in the following two ways: The first effect is that the maximum phonon energy participating in the phonon drag effect, which is given by $2\hbar v_s k_F$ (v_s is the velocity of sound and k_F is the Fermi momentum), is larger than $k_0 T$ in the temperature range in which we are interested. On the other hand, in pristine graphite $2\hbar v_s k_F / k_0$ is at most ~ 40 K. The second effect is as follows. The q-dependent scattering processes, for instance, the carrier-phonon scattering, Rayleigh scattering, and phonon-phonon scattering provide large relaxation rates in the phonon-relaxation processes. Among them the Rayleigh scattering, due to point defects, is strongly enhanced as compared with the case of pristine graphite, since its relaxation rate $1/t_I(q)$ is proportional to q^3 in two-dimensional phonons and to q^4 in three-dimensional cases. At temperatures above ~ 100 K, the Rayleigh scattering plays an important role in the phonon-relaxation process, and by combining the diffusion term with the phono drag term, the overall features of the TEP in the acceptor compounds are qualitatively explained. Detailed calculations are carried out by solving the coupled Boltzmann equations for carriers and phonons.

II. ELECTRON-PHONON INTERACTION

A. Diffusion contribution to TEP

The TEP is composed of the two contributions: The diffusion term S_d and the phonon drag term S_p, $S = S_d + S_p$. We will first evaluate S_d. To be more definite, let us consider the stage-2 acceptor compound, which can be treated on the basis of the band model of Blinowksi et al.[11]

In the presence of an electric field $\vec{F}$ and a temperature gradient $\vec{\nabla} T$, the current density $\vec{j}$ and heat-current density $\vec{w}$ are expressed as follows:

$$\vec{j} = \sigma\vec{F} - \beta\vec{\nabla}T, \quad \vec{w} = \chi\vec{F} - \zeta\vec{\nabla}T . \tag{1}$$

Between the transport coefficients σ, β, χ, and ζ there exists Onsager's relations,

$$\sigma_{ij}(H) = \sigma_{ji}(-H) , \tag{2a}$$

$$T\beta_{ij}(H) = \chi_{ji}(-H) , \tag{2b}$$

$$\zeta_{ij}(H) = \zeta_{ji}(-H) . \tag{2c}$$

In the absence of a magnetic field H, the TEP is given by

$$S = \beta_{xx}/\sigma_{xx} = \chi_{xx}/T\sigma_{xx} . \tag{3}$$

Theoretically, it is easier to calculate χ_{xx} than β_{xx},[7-10] so that in the following we may set $\vec{\nabla}T = \vec{0}$. χ_{xx} and σ_{xx} are given by

$$\chi_{xx} = -e \sum \sum v_{ix}^2 \tau_i (E_i(k) - E_F) \partial f_0/\partial E_i , \tag{4}$$

$$\sigma_{xx} = -e^2 \sum \sum v_{ix}^2 \tau_i \partial f_0/\partial E_i ,$$

where v_{ix} denotes the velocity component along the x axis of the ith band and τ_i is the relaxation time. χ_{xx} and σ_{xx} may be rewritten in the form,

$$\chi_{xx} = \frac{e(\pi k T)^2}{3\pi I_c} \sum_i \left[\frac{d}{dE_i} \left[\frac{dk_i}{dE_i}(k_i v_{ix}^2 \tau_i) \right] \right]_{E_i = E_F} ,$$

$$\sigma_{xx} = \frac{e^2}{\pi I_c} \sum_i \left[\frac{dk_i}{dE_i}(k_i v_{ix}^2 \tau_i) \right]_{E_i = E_F} , \tag{5}$$

where $v_i^2 = v_{ix}^2 + v_{iy}^2$. Then S_d becomes

$$S_a = \frac{\pi^2 k_0^2}{3e} T \frac{\sum_i \left[\frac{d}{dE_i} \left[\frac{dk_i}{dE_i}(k_i v_{ix}^2 \tau_i) \right] \right]_{E_i = E_F}}{\sum_i \left[\frac{dk_i}{dE_i}(k_i v_{ix}^2 \tau_i) \right]_{E_i = E_F}} . \tag{6}$$

The band structure of the stage-2 acceptor compound is shown in Fig. 3, and the two hole bands 1 and 2 (v_1 and v_2 are abbreviated by 1 and 2) are given by[11]

$$E_1(k) = \frac{1}{2}[\gamma_1 - (\gamma_1^2 + 9\gamma_0^2 b^2 k^2)^{1/2}] ,$$

$$E_2(k) = \frac{1}{2}[-\gamma_1 - (\gamma_1^2 + 9\gamma_0^2 b^2 k^2)^{1/2}] , \tag{7}$$

where $k^2 = k_x^2 + k_y^2$ and b denote the nearest C-C distance (1.42 Å). Since $3\gamma_0 b k_F \gg \gamma_1$,[11,12] Eq. (7) leads to

$$v_i^2 \cong (A/\hbar)^2, \quad dk_i/dE_i \cong 1/A, \quad A \equiv \frac{3}{2}\gamma_0 b . \tag{8}$$

Accordingly, Eq. (6) becomes

$$S_d \cong \frac{\pi^2 k_0^2 T}{3e} \frac{\sum_i [(d/dE_i)(E_i \tau_i)]_{E_i = E_f}}{\sum_i (E_i \tau_i)_{E_i = E_F}} . \tag{9}$$

Assuming $\tau_i(E_i) \propto E_i^p$, we get
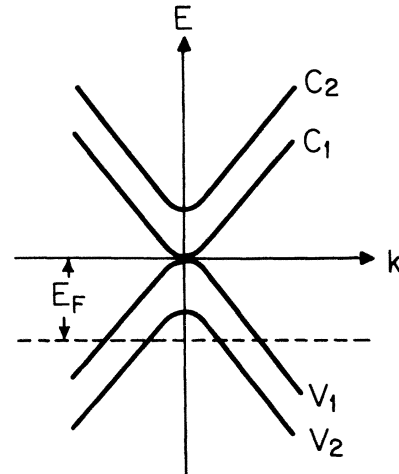
$$S_d \cong (\pi^2/3e)(k_0^2 T/E_F)(1 + P) , \tag{10}$$

FIG. 3. Band structure of the stage-2 acceptor compounds (Ref. 11).

THERMOELECTRIC POWER OF GRAPHITE INTERCALATION . . .

where p depends on the scattering mechanism. If $E_F = 0.7$ eV is inserted into Eq. (10), we obtain

$$S_d \cong 3.50(1+P) \times 10^{-2}T , \tag{11}$$

measured in $\mu V/K$, which is in good agreement with the observed value of $3.0 \times 10^{-2}T(\mu V/K)$ for the stage-2 $SbCl_5$-intercalated graphite.[6] Equation (11) yields too small a value of S_d to explain the observed TEP at high temperatures. However, it should not be neglected.

B. Scattering due to the in-plane vibration

Electron-phonon interaction is assumed to be in the following form:

$$H_{e\text{-ph}} = \sum_q V_q (b_q^\dagger e^{iqr} - b_q e^{iqr}) ,$$

$$V_q = -iD(\hbar/2d\Omega\omega_q)^{1/2}q \tag{12}$$

(Ω is the volume of crystal and d is the density), where the in-plane vibration interacts most strongly with carriers and the dispersion relation is approximately given by

$$\omega_q = v_s q, \quad q^2 = q_x^2 + q_y^2 \tag{13}$$

$(v_s = 2.1 \times 10^6$ cm/sec). We disregard the potential exerted on the carriers in the graphite layers by the ionized intercalated layers. Recently, Giergiel et al. revealed that low-frequency phonon modes with a large density of states exist in stage-2 graphite rubidium.[13] These modes are ascribed to the vibrations of the intercalated layers. These modes might be related to the anomalous behavior of the TEP in a stage-5 graphite-potassium compound. (See Fig. 4, lower panel.) In this paper we do not go deeply into the calculation for the TEP in donor compounds. Equations (12) and (13) are essentially equivalent to the case of graphite.[14]

The coupling constant D has three components associated with the three transitions $1 \to 1'$, $2 \to 2'$, and $1 \leftrightarrow 2$. Here we assume that

$$D_{11} = D_{22} \equiv D, \quad D_{12} = D_{21} \equiv D' . \tag{14}$$

In general, $D_{11} \neq D_{22}$, however, if $2E_F$ is larger than γ_1, D_{11} is approximately equal to D_{22}. As is shown in the Appendix, the intraband transition term D is much larger than the interband contribution D'. Therefore, in the following, D' is neglected. From Eq. (12) the relaxation rate τ_{11} is represented as follows:

$$\frac{1}{\tau_{11}(E)} = \frac{\pi D^2}{d\Omega v_s} \sum_q q N_{q_0} \left[\frac{q_x}{k_x} \delta(E_1(k+q) - E_1(k) - \hbar\omega_q) \frac{f_0(E_1(k)+\hbar\omega_q)}{f_0(E_1(k))} e^{\beta\hbar\omega_q} \right.$$

$$\left. + \frac{q_x}{k_x} \delta(E_1(k-q) - E_1(k) + \hbar\omega_q) \frac{f_0(E_1(k)-\hbar\omega_q)}{f_0(E_1(k))} \right] . \tag{15}$$

For simplicity, we assume that

$$\frac{f_0(E_1(k)+\omega_q)}{f_0(E_1(k))} e^{\beta\hbar\omega_q} \cong 1, \quad N_{q_0} \cong \frac{k_0 T}{\hbar\omega_q} ,$$

$$\delta(E_1(k \pm q) - E_1(k) \mp \hbar\omega_q) \cong \delta(E_1(k \pm q) - E_1(k)) . \tag{16}$$

Equation (16) is a high-temperature approximation. In the temperature region of interest $(T \sim 300$ K), the above approximation is not valid since $2\hbar v_s k_F > k_0 T$. From Eqs. (15) and (16), we get

$$\frac{1}{\tau_{11}(E)} \cong \frac{D^2 k_0 T}{2\pi I_c d\hbar v_s^2}$$

$$\times \int dq \, d\phi_q q [\delta(E_1(k+q) - E_1(k))$$

$$+ \delta(E_1(k-q) - E_1(k))] , \tag{17}$$

where I_c denotes the period of the crystal along the c axis. By using Eq. (7), we obtain

$$\frac{1}{\tau_{11}(E)} \cong \frac{D^2 k_0 T(|E_1| + \frac{1}{2}\gamma_1)}{d\hbar v_s^2 A^2 I_c} . \tag{18}$$
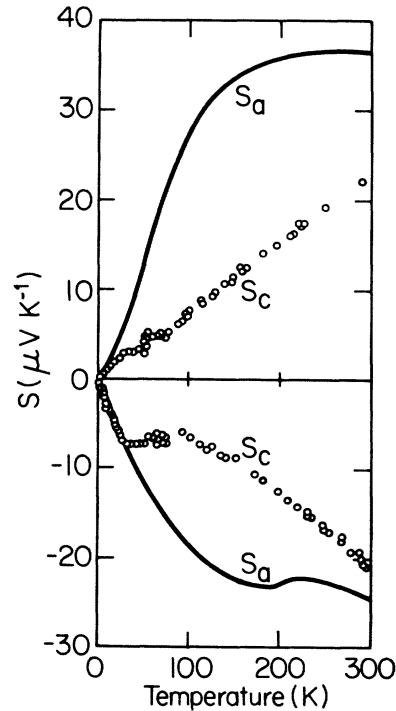
Similarly, $1/\tau_{22}(E)$ becomes

FIG. 4. Temperature variation of the c-axis TEP S_c of stage-2 $FeCl_3$-intercalated graphite and stage-5 potassium-intercalated graphite compounds. For comparison, the in-plane TEP S_a are also represented (Ref. 5).

$$\frac{1}{\tau_{22}(E)} \cong \frac{D^2 k_0 T(|E_2|-\frac{1}{2}\gamma_1)}{d\hbar v_s^2 A^2 I_c} . \tag{19}$$

To get an order-of-magnitude estimate of the carrier-relaxation time, we insert the following set of parameters into Eqs. (18) and (19):

$$D=16, \quad |E_1|=|E_2|=E_F=0.7, \quad \gamma_1=0.3 ,$$

measured in eV (Ref. 14),

$$\gamma_0=3, \quad d=2, \quad v_s=2.1\times10^6, \quad I_c=8.75 , \tag{20}$$

where γ_0 is measured in eV, v_s is measured in cm/sec (Ref. 14), and I_c is measured in Å,[1] then at 300 K, τ_{11} and τ_{22} become

$$\tau_{11}=2.3\times10^{-13}, \quad \tau_{22}=3.6\times10^{-13} , \tag{21}$$

measured in sec. These values for the carrier-relaxation times give rise to the mobility values

$$\mu_1=3000, \quad \mu_2=4780 \tag{22}$$

measured in cm^2/V sec. Apart from numerical factors, Eq. (22) gives the correct order of the observed mobilities.[1] $D=16$ eV is the value in pristine graphite.[14] As already mentioned, Eqs. (18) and (19) are derived by using the high-temperature approximation $2\hbar v_s k_F/k_0 T < 1$, which is not valid for $T < 300$ K. Therefore it is necessary to calculate the conductivity on the basis of a variational principle and determine the magnitude of the coupling constant D in comparison with the observed data.

III. PHONON DRAG CONTRIBUTION TO THE TEP

The distribution function for carriers and phonons is governed by the following Boltzmann equation:

$$e(\vec{F}\cdot\vec{v}_i)\frac{\partial f_i}{\partial E_i} = \left[\frac{\partial f_i}{\partial t}\right]_{coll} \quad (e>0), \quad i=1,2$$

$$\left[\frac{\partial N_q}{\partial t}\right]_{carrier} - \frac{N_q-N_{q0}}{t_r}=0 , \tag{23}$$

where for convenience the hole bands 1 and 2 are inverted, f_i is the distribution function for the ith band, $(\partial N_q/\partial t)_{carrier}$ denotes the change of the phonon distribution function due to collision with carriers, and t_r represents the phonon-relaxation time resulting from all scattering processes except the phonon-carrier scattering. $(\partial f_i/\partial t)_{coll}$ is composed of the two terms

$$\left[\frac{\partial f_i}{\partial t}\right]_{coll} = \left[\frac{\partial f_i}{\partial t}\right]_{phonon} - \frac{f_i-f_{i0}}{\tau_r} , \tag{24}$$

where τ_r indicates the carrier-relaxation time including all scattering processes except the scattering due to the in-plane phonons. Let us assume f_i and N_q have the following forms:

$$f_i=f_{i0}-[V_i(E)\hbar k]\frac{\partial f_{i0}}{\partial E}, \quad N_q=N_{q0}-[U(\omega_q)q]\frac{\partial N_{q0}}{\partial \omega_q} , \tag{25}$$

where $(\partial N_q/\partial t)_{carriers}$ is written as follows[7-9]:

$$\left[\frac{\partial N_q}{\partial t}\right]_{carrier} = -(N_q-N_{q0})t_c^{-1}+(q^2/\Omega\omega_q)2\times2\beta N_{q0}$$

$$\times \sum_i \alpha_{ii} \sum_{k,k'} \{[V_i(E')\hbar k']-[V_i(E)\hbar k]\}$$

$$\times\delta(E_i(k')-E_i(k)-\hbar\omega_q)\delta_{k',k+q}f_{k0}(1-f_{k',0}) \quad (\beta\equiv1/k_0T) \tag{26}$$

where $\alpha_i \equiv \pi D_{ii}^2/d=\pi D^2/d$, and the relaxation time t_c due to the collision with carriers takes the form

$$\frac{1}{t_c} = \frac{4q^2}{\Omega\omega_q(N_{q0}+1)}\sum_\lambda \alpha_{\lambda\lambda}\sum_{k,k'}\delta(E_i(k')-E_i(k)-\hbar\omega_q)\delta_{k',k+q}f_{k0}(1-f_{k'0})=\sum_i\frac{1}{t_{ii}} . \tag{27}$$

Equation (27) is calculated as follows:

$$\frac{1}{t_{ii}} \cong \frac{\alpha_{ii}\hbar q k_{Fi}}{\pi I_c A^2} \propto q , \tag{28}$$

where k_{Fi} is the Fermi momentum of the ith band. $(\partial N_q/\partial t)_{carrier}$ is rewritten as

$$\left[\frac{\partial N_q}{\partial t}\right]_{carrier} = -(N_q-N_{q0})t_c^{-1}+\beta N_{q0}(N_{q0}+1)\sum_i\frac{V_i\hbar q}{t_{ii}(q)} , \tag{29}$$

where we employ the approximation of $V_i(E)=V_i(E_F)\equiv V_i$. \tag{30}

In the case of $\alpha_{ij}\neq0$ for $i\neq j$, Eq. (29) should be replaced by

$$\left[\frac{\partial N_q}{\partial t}\right]_{carrier} = -(N_q-N_{q0})t_c^{-1}+\beta N_{q0}(N_{q0}+1)\sum_{i,j}\frac{(V_j\hbar q)[1+Q_{ij}(q)]1}{t_{ij}(q)} , \tag{31}$$

where

$$Q_{ij}(q)=\frac{k_{Fj}^2-k_{Fi}^2}{q^2}, \quad \frac{1}{t_c}=\sum_{i,j}\frac{1}{t_{ij}},$$

$$\frac{1}{t_{ij}}=\frac{\alpha_{ij}\hbar q(k_{Fi}k_{Fj})^{1/2}}{\pi I_c A^2}. \tag{32}$$

Inserting Eqs. (25) and (30) into (23), we get[7-9]

$$U(\omega_q)=\sum R_{ii}(q)V_i, \quad R_{ii}(q)=\frac{t(q)}{t_{ii}(q)}<1,$$

$$\frac{1}{t}=\frac{1}{t_c}+\frac{1}{t_r}. \tag{33}$$

Similarly, Eq. (24) is written as

$$\left[\frac{\partial f_i}{\partial t}\right]_{coll}=\frac{-(f_i-f_{i0})}{\tau_i}+\left[\frac{\partial f_i}{\partial t}\right]_{drag},$$

$$\frac{1}{\tau_i}=\frac{1}{\tau_{ir}}+\frac{1}{\tau_{ip}}, \quad \frac{1}{\tau_{ip}}\cong\frac{1}{\tau_{ii}}. \tag{34}$$

τ_{ip} is the relaxation time of ith band carriers associated with in-plane phonon scattering. Since we disregard interband transitions, τ_{ip} is nearly equal to τ_{ii} and $(\partial f_i/\partial t)_{drag}$ is represented by

$$\left[\frac{\partial f_i}{\partial t}\right]_{drag}=-\frac{\hbar\tau_{ip}^{-1}}{4k_{Fi}^4}\int_0^{2k_{Fi}}dq\,q^3[U(\omega_q)k]\frac{\partial f_{i0}(k)}{\partial E}.$$

$$\tag{35}$$

In deriving Eq. (35), we assume that the carrier system has a three-dimensional band represented by $E=\hbar^2k^2/2m$.

From Eqs. (35), (33), and (23) the coupled equations for V_i are obtained,

$$V_i[1-\Gamma(i,i)]-\sum_{i\neq j}\Gamma(i,j)V_j=\mu_i F, \tag{36}$$

where

$$\Gamma(i,j)=\frac{r_i}{4k_{Fi}^4}\int_0^{2k_{Fi}}dq\,q^3R_{jj}(q), \quad r_i\equiv\frac{\tau_i}{\tau_{ip}}<1. \tag{37}$$

$\Gamma(i,j)$ is called the "mutual drag coefficient" which was first introduced by Gurevich and Korenblit[15] in their study of thermoelectric and thermomagnetic effects. μ_i denotes the mobility of the ith carrier in the case of $N_q=N_{q0}$. Since r_i and R_{jj} are both smaller than unity, then we have $\Gamma(i,j)<1$. $\Gamma(i,j)$ is usual neglected in treating thermoelectric and thermomagnetic effects,[7-9,15] though sometimes it plays an important role. The mobility μ_M of highly oriented pryolytic graphite defined by $\lim(H\to0)C(\Delta\rho/\rho_0H^2)^{1/2}$ is proportional to $T^{-1.6}$ between 40 and 80 K, and to $T^{-1.2}$ above 80 K. The $T^{-1.2}$ dependence was observed by Soule[16] and it is in good agreement with our theory.[14] The change from a $T^{-1.2}$ dependence to a $T^{-1.6}$ dependence is caused by the mutual drag effect.[17] A similar temperature dependence of μ_M was also observed by Kreps and Woollam.[18]

We will not enter into the detailed consideration on $\Gamma(i,j)$. Equations (33) and (36) are the basic equations describing the thermoelectric effect in the presence of a deviation of the phonon distribution from equilibrium.[7-9,15] Now we can easily extend these equations to the

higher-stage compounds, because Eqs. (33) and (36) are general expressions which are not limited to the two-carrier system.

Solving the simultaneous equations on V_1 and V_2, we obtain (N_1,N_2 are the carrier concentrations)

$$\sigma_{xx}=e\sum_i N_i\mu_i^*$$

$$\mu_i^*=\{\mu_1[1-\Gamma(2,2)]+\mu_2\Gamma(1,2)\}/\Delta,$$

$$\mu_2^*=\{\mu_2[1-\Gamma(1,1)]+\mu_1\Gamma(2,1)\}/\Delta, \tag{38}$$

$$\Delta=[1-\Gamma(1,1)][1-\Gamma(2,2)]-\Gamma(1,2)\Gamma(2,1).$$

Now we are ready to calculate the phonon drag TEP. The heat-current density associated with the phonon system is given by

$$w_x=\sum_q \hbar\omega_q V_x(q_x/q)(N_q-N_{q0}),$$

$$N_q-N_{q0}=-[U(\omega_q)q](\partial N_{q0}/\partial\omega_q). \tag{39}$$

Referring to Eq. (33), w_x becomes

$$w_x=\frac{\beta(\hbar v_s)^2}{4\pi I_c}\int dq\,q^3 N_{q0}(N_{q0}+1)\sum_i R_{ii}(q)V_i. \tag{40}$$

Inserting Eq. (38) into (40), we obtain

$$\chi_{xx}^p=\frac{\beta(\hbar v_s)^2}{4\pi I_c}\int dq\,q^3 N_{q0}(N_{q0}+1)\sum_i \mu_i^* R_{ii}. \tag{41}$$

Therefore the phonon drag TEP takes the form

$$S_p=\frac{\beta(\hbar v_s)^2}{4\pi I_c}\int dq\,q^3 N_{q0}(N_{q0}+1)$$

$$\times\left[\sum_i \mu_i^* R_{ii}\right]\left[\sum_i eN_i\mu_i^*\right]^{-1}. \tag{42}$$

In expression (42), the temperature dependence of μ_i^* in the denominator and numerator cancel each other. Accordingly, the behavior of S_p is determined by the T and q dependence of $R_{ii}(q)=t(q)/t_{ii}(q)$. An explicit expression for $t_{ii}(q)$ has already been given by Eq. (28); however, the information on $t(q)$ is needed to evaluate Eq. (42).

IV. TEMPERATURE DEPENDENCE OF THE PHONON DRAG TEP

The total phonon relaxation rate $1/t$ is represented by

$$\frac{1}{t}=\frac{1}{t_b}+\frac{1}{t_c}+\frac{1}{t_I}+\frac{1}{t_p}, \tag{43}$$

where (i) $1/t_b$ is due to boundary scattering, $1/t_b\cong v_s/L\equiv b$, where L is the sample dimension; (ii) $1/t_c$ is due to the carrier-phonon scattering process given by Eq. (28), namely $1/t_c=aq$; (iii) $1/t_I$ is due to Rayleigh scattering associated with point defects. For two-dimensional phonons, $1/t_I(q)=fq^3$; (iv) $1/t_p$ is due to the phonon-phonon scattering process, which for two-dimensional phonons has the functional form $1/t_p=BqT^3$.[7-9] In the following, $\Gamma(i,j)$ is neglected.

According to (i)-(iv), the temperature range is divided into the following regions.

(1) Very low temperatures: $2\beta\hbar v_s k_F \gg 1$. In this region, the boundary scattering is the predominant process. Then we have $R \cong t_b/t_c \propto q$. From Eq. (42), we get $S_p \propto T^3$ and this temperature variation was confirmed in $SbCl_5$-intercalated graphite compounds up to 20 K.[6] An estimate for $1/t_c$ can be obtained from Eq. (28). Since the carrier densities in GIC are 1 or 2 orders of magnitude larger than that of pristine graphite, the screening effect on the electron-phonon interaction due to carriers is more important in GIC. Therefore it is expected that $D(\text{GIC}) < D(\text{graphite})$. Tentatively, let us assume that $D = 10$ eV.

Substituting the values $\gamma_0 = 3$ eV, $k_f = 2 \times 10^7$ cm^{-1}, $d = 2$, and $q = 10^6$ cm^{-1} ($\hbar v_s q/k_0 = 16$ K) into Eq. (28), we get $1/t_{ii} = 2.95 \times 10^9$ sec^{-1}. If we take a value $L = 10^{-4}$ cm, $1/t_b$ becomes $v_s/L = 2.1 \times 10^{10}$ sec^{-1}. Then the relation of $t_b \ll t_c$ is satisfied at very low temperatures.

(2) Low temperatures: $2\beta\hbar v_s k_F \gg 1$. In this case the phonon-relaxation rate is approximately given by

$$\frac{1}{t} \cong \frac{1}{t_b} + \frac{1}{t_c} ,$$

where   (44)

$$\frac{1}{t_b} \sim \frac{1}{t_c} .$$

Therefore $R \propto q^p$, where $0 < p < 1$ and then $S_p \propto T^{2+p}$. However, it should be noted that in this case the mutual drag coefficients $\Gamma(i,j)$ cannot be neglected (since they are not small compared with unity) and the situation will become complicated.

(3) Intermediate temperatures: $\exp(2\beta\hbar v_s k_F) \gg 1$. In this region $1/t$ is represented by

$$\frac{1}{t} \cong \frac{1}{t_I} + \frac{1}{t_c} + \frac{1}{t_p} ,$$ (45)

and we assume that the inequality $1/t_I \gg 1/t_c$, $1/t_p$ is satisfied. Dreyfus and Maynard[19] analyzed the thermal conductivity measurement in graphite and obtained

$$\frac{1}{t_I} = fq^3, \quad f = 8.63 \times 10^{-14} ,$$

measured in sec^{-1}cm^3,   (46)

$$\frac{1}{t_p} = BqT^3, \quad B = 2.65 \times 10^{-5} ,$$

measured in cm/sec K^3.

However, they did not take into consideration the relaxation process due to the electron-phonon interaction. By introducing a simple two-ellipsoid model, the phonon-relaxation rate related to the carrier scattering is obtained as follows[7-9]:

$$\frac{1}{t_{ij}} = \frac{D^2 \hbar q}{\pi d} \frac{m_\perp^{(i)} m_\perp^{(j)}}{h^4} \xi ,$$ (47)

where $m_\perp^{(i)}$ denotes the effective mass in the basal plane of the ith band (electron or hole) and

$$\xi \cong (m_\parallel^{(e)}/m_\perp^{(e)})^{1/2} \cong (m_\parallel^{(k)}/m_\perp^{(h)})^{1/2} \cong 12.1 .$$

Inserting $D = 16$ eV, $m_\perp^{(e)} = 0.057 m_0$, $m_\perp^{(h)} = 0.039 m_0$, and $q = 2 \times 10^6$ cm^{-1} into Eq. (47), we get

$$\frac{1}{t_{ij}} = \begin{cases} 2.41 \times 10^9, & i = j = h \\ 5.16 \times 10^9, & i = j = e \end{cases}$$ (48)

measured in sec^{-1}. Substituting $q = 2 \times 10^6$ cm^{-1} and $T = 200$ K into Eq. (46), we get

$$\frac{1}{t_I} = 8 \times 10^5$$

and   (49)

$$\frac{1}{t_p} = 4.24 \times 10^8 ,$$

measured in sec^{-1}. These values are much smaller than Eq. (48). Therefore it is very necessary to consider the phonon-carrier scattering process in analyzing the thermal conductivity data in pristine graphite. On the other hand, Kelly[20] obtained

$$\frac{1}{t_I} = 6.18 \times 10^9 ,$$ (50)

measured in sec^{-1} at $T = 200$ K. This value is very much larger than the one obtained by Dreyfus and Maynard.[19] In the recent measurements on the thermal conduction in FeCl$_3$- and K-intercalated graphite, Issi et al.[21] employed the same parameters for $1/t_I$ and $1/t_p$ as those of graphite.[19]

In the case of GIC, there are many reasons why the Rayleigh scattering is important. By introducing intercalant layers into pristine graphite, it is expected that many point defects are formed. Owing to the functional dependence of $1/t_I(q) \propto q^3$, the Rayleigh scattering becomes the predominant process at high temperatures in GIC with a large cross-sectional diameter of the Fermi surface ($k_F \sim 10^7$ cm^{-1}).

Now let us return to the estimation of the TEP. From Eq. (42), the T dependence of the phonon drag TEP is given by

$$S_p \propto T^{-2} \int_{q_0}^{q_{max}} dq \, q^3 N_{q_0}(N_{q_0}+1)R$$

$$\propto T^{-2} \int_{q_0}^{q_{max}} dq \, q N_{q_0}(N_{q_0}+1) ,$$ (51)

where $q_{max} = 2k_F$ and the lower limit q_0 is estimated by the condition

$$\frac{1}{t_I} = \frac{1}{t_c} + \frac{1}{t_p} .$$ (52)

Namely, we have

$$q_0 = (a/f + BT^3/f)^{1/2} .$$ (53)

If the condition of $1/t_I \gg 1/t_c, 1/t_p$ for $\hbar v_s q \sim k_0 T$ is satisfied, we get

$$\beta\hbar v_s q_0 \equiv x_0 \equiv (\hbar v_s/k_0)(a/fT^2 + BT/f)^{1/2} < 1 ,$$

and since

$$\exp(\beta\hbar v_s q_{max}) \equiv \exp(\beta x_m) \gg 1 ,$$

Eq. (51) is approximated by

$$S_p \propto \int_{x_0}^{x_{max}} dx \, x \frac{e^x}{(e^x-1)^2} \cong -\ln x_0 + \int_1^\infty \frac{dx}{e^x-1}$$

$$= -\ln x_0 + 0.46 .$$ (54)

In the case of $a/fT^2 > BT/f$, S_p slowly increases with T, while in the region of $a/fT^2 < BT/f$, S_p slightly decreases with T. By adding to S_p the diffusion term S_d, which is a few $\mu V\,K^{-1}$ at $T > 100$ K, the resultant $S = S_d + S_p$ exhibits a weak temperature dependence. This behavior is in qualitative agreement with the observed results shown in Figs. 1 and 2.

V. DISCUSSION

On the basis of the above calculations, we can understand that the reason why the TEP of GIC and graphite behave differently is due to differences in their Fermi surfaces. The diameter of the Fermi-surface cross section in graphite is at most $\sim 10^6$ cm^{-1}, while the corresponding value in GIC is $\sim 10^7$ cm^{-1}.[1] Thus in GIC the Rayleigh scattering becomes very important in the phonon-relaxation processes, while in graphite this process plays a minor role. The many point defects introduced in the intercalation process further enhance the importance of the Rayleigh scattering.

Figures 1 and 2 show that the observed TEP values are weakly dependent on stage except for stage-10 SbCl$_5$-intercalated graphite, which is a weakly degenerate system. This feature can be qualitatively explained by the basis of Eq. (42). For simplicity, we assume $\mu_i^* = \mu_0^*$; then Eq. (42) becomes

$$S_p \cong \frac{\beta(\hbar v_s)^2}{4\pi I_c TNe} \int dq\, q^3 N_{q_0}(N_{q_0}+1)R , \qquad (55)$$

where

$$R = \sum_i R_{ii} = \sum_i \frac{t(q)}{t_{ii}(q)} = \frac{t(q)}{t_c(q)}$$

and $N = \sum_i N_i$.

The repeat distance I_c is related to c_0 (interlayer graphite distance) by[1]

$$I_c = d_s + (n-1)c_0 \qquad (56)$$

(n is the stage index), where d_s is in most cases essentially independent of stage for $n \geq 2$.[1] Since the carrier density is roughly inversely proportional to stage-index n, I_c is nearly constant. t_f and t_c are expected to increase with n, so that $R = t(q)/t_c(q)$ is considered to be insensitive to stage in the intermediate-temperature range. Therefore S_p is roughly stage independent.

In the following we will derive the ratio S_p/S_d from simple considerations. As is well known, the phonon drag TEP can be represented by the following simple formula[7]:

$$S_p = \frac{\langle C_p R \rangle}{3eN} , \qquad (57)$$

where C_p denotes the heat capacity of the phonon system participating in the phonon drag effect. In the present problem $\langle C_p R \rangle$ takes the form

$$\langle C_p R \rangle = \frac{2\pi}{I_c}\frac{2\pi}{(2\pi)^3} \int_0^{2k_F} dq\, q\frac{(\hbar\omega_q)^2}{k_0 T^2} N_{q_0}(N_{q_0}+1)R(q) . \qquad (58)$$

Rewriting Eq. (58), we get

$$\langle C_p R \rangle = \frac{k_0 q_T^2}{2\pi I_c} \int_0^{x_{max}} dx\, x^3\frac{e^x}{(e^x-1)^2}R(x) , \qquad (59)$$

where $\hbar v_s q_T = k_0 T$ and $x_m = 2v_s k_F/k_0 T$. The carrier density N is given by

$$N = \frac{2\times 2}{(2\pi)^3}\frac{2\pi}{I_c}\sum_c \pi k_{F_i}^2 = \frac{1}{\pi I_c}\sum_i k_{Fi}^2 . \qquad (60)$$

Then we get

$$S_p \cong \frac{k_0}{6e}\left[\frac{q_T}{k_F}\right]^2 R_0 J_4, \quad J_4 = \int_0^\infty dx\frac{x^4 e^x}{(e^x-1)^2} \cong 26 . \qquad (61)$$

Here we consider the low-temperature region where the phonon relaxation is mainly controlled by the boundary scattering.

Then

$$R(q) \cong \frac{t_b}{t_c} = at_b q_T x = \left[\frac{q_T}{q_0}\right]x = R_0 x , \qquad (62)$$

where $aq_0 \equiv t_b^{-1}$. With the use of Eq. (10), S_p/S_d is given by

$$\frac{S_p}{S_d} \cong \frac{J_4}{2\pi^2}R_0\left[\frac{q_T}{k_F}\right]^2\frac{T_F}{T}, \quad k_0 T_F \equiv E_F . \qquad (63)$$

Inserting $k_F \cong 2\times 10^7$ cm^{-1}, $T_F = 8120$ K ($E_F = 0.7$ eV), $T = 30$ K, and Eq. (28) with $D = 10$ eV into Eq. (63), we get

$$S_p/S_d \cong 0.88$$

then

$$S_p \approx S_d . \qquad (64)$$

This is in qualitative agreement with the observed value in Fig. 2 for stage-2 SbCl$_5$-intercalated graphite. At high temperatures we can also show that $S_p > S_d$.

In Fig. 4 the temperature variation of the TEP in stage-5 potassium GIC is shown.[5] This behavior is different from those in the acceptor compounds. It may be related to the phonon drag effect associated with the low-frequency phonon modes with a large density of states in the donor compounds.[13] These modes are ascribed to the vibrations of the intercalated layers.[13]

Elzinga *et al.* measured the magnetothermoelectric power of SbCl$_5$-intercalated graphite samples up to 6 T and ascertained that the effect of a magnetic field is very weak.[6] Investigation of the magnetothermoelectric power and Nernst-Ettingshausen effect over a wide range of temperatures and field strengths will provide useful information, then it is highly desirable to study the thermomagnetic effects.

APPENDIX

To get an expression of the electron-phonon interaction, the rigid-ion approximation is employed (see Ref. 14, Sugihara and Sato).

The perturbing potential is

$$H' = \sum_j \sum_\alpha [V(\vec{r} - \vec{R}_{j\alpha} - \vec{\xi}_{j\alpha}) - V(\vec{r} - \vec{R}_{j\alpha})]$$

$$= -\sum_j \sum_\alpha \vec{\xi}_{i\alpha} \cdot \vec{\nabla} V_{j\alpha} , \qquad (A1)$$

where $V(\vec{r} - \vec{R}_{j\alpha})$ is the potential energy of an electron due to the ion $(j\alpha)$, $\vec{\xi}_{j\alpha}$ denotes the displacement of the lattice point $\vec{R}_{j\alpha}$ from the equilibrium position, j represents the jth unit cell, and α is the nonequivalent carbon atoms in a unit cell.

Introducing normal coordinates for $\vec{\xi}_{j\alpha}$, we have to evaluate integrals of the type

$$\int \Psi_{t'}^*(\vec{k}') \left[\sum_j \sum_\alpha e^{\pm i \vec{q} \cdot \vec{R}_{j\alpha}} \hat{e}_{q\lambda} \cdot \vec{\nabla} V_{j\alpha} \right] \Psi_t(\vec{k}) d\tau , \qquad (A2)$$

where t and t' are suffixes specifying the electron states and $e_{q\lambda}$ is the polarization vector of a phonon belonging to the λth mode.

In the case of the stage-2 acceptor compounds, we diagonalize the two-layer Hamiltonian in the subspace spanned by[11]

$$U_{ik}(\vec{r}) = N^{-1/2} \sum_n e^{i\vec{k} \cdot \vec{R}_n} \psi_z(\vec{r} - \vec{R}_n), \quad i = A, B, A', B' , \qquad (A3)$$

where the summation is carried out over one type of the equivalent carbon atom sites. Namely, the summation over n is equivalent to the summation over j in Eq. (A1) for a fixed α. A and B are located in the first layer, while A' and B' lie in the second layer. The nearest A-A' distance is equal to $C_0/2 = 3.354$ Å. In the tight-binding approximation, ψ_z represents the $2P_z$ orbital. Wave functions corresponding to the two hole bands v_1 and v_2 are[11]

$$\Psi_1 = [(2E_1)^{1/2}(\gamma_1^2 + 9\gamma_0^2 b^2 k^2)^{1/4}]^{-1}$$

$$\times (E_1 U_{Ak} + \gamma_0 g^* U_{Bk} + E_1 U_{A'k} + \gamma_0 g U_{B'k}) ,$$

$$\Psi_2 = [(2E_2)^{1/2}(\gamma_1^2 + 9\gamma_0^2 b^2 k^2)^{1/4}]^{-1} \qquad (A4)$$

$$\times (E_2 U_{Ak} + \gamma_0 g^* U_{Bk} - E_2 U_{A'k} - \gamma_0 g U_{B'k}) ,$$

where $g \cong \frac{3}{2} bk \exp(-i\theta)$, $\tan\theta = k_y/k_x$.

Similarly, the electron wave functions are easily written down.[11] If the potential in one unit cell is mainly due to the ion in the cell, Eq. (A2) becomes

$$\sum_\alpha \int \hat{e}_{q\lambda} \cdot \vec{\nabla} V(\vec{r} - \vec{R}_\alpha) \exp[\mp i \vec{q} \cdot (\vec{r} - \vec{R}_\alpha)]$$

$$\times u_{t'}^*(\vec{k}') u_t(\vec{k}) d\tau_0 , \qquad (A5)$$

where $\alpha = A, B, A', B'$, $\Psi_t = N^{-1/2} \exp(i\vec{k} \cdot \vec{r}) u_t(\vec{k})$, $t = 1$ or 2, and $d\tau_0$ is the integral over a unit cell. In deriving Eq. (A5), conservation of the wave vectors $\vec{k} - \vec{k}' \pm \vec{q} = 0$ is employed. Assuming $\psi_z(\vec{r} - \vec{R})$ and $V(\vec{r} - \vec{R})$ are well localized around the lattice point $\vec{R}$, we can use the approximation

$$\left| \int U_{i',k'}^*(\vec{r}) \vec{\nabla} V(\vec{r} - \vec{R}_\alpha) U_{ik}(\vec{r}) d\tau_0 \right| \ll \left| \int U_{i'k'}^*(\vec{r}) \vec{\nabla} V(\vec{r} - \vec{R}_i) U_{ik}(\vec{r}) d\tau_0 \right| , \qquad (A6)$$

for $\alpha \neq i'$ or i or $i' \neq i$. Therefore, by inspection of Eq. (A4), we get the relation

$$\sum_j \sum_\alpha e^{\pm i \vec{q} \cdot \vec{R}_{j\alpha}} \int \Psi_1^* \vec{\nabla} V_{j\alpha} \Psi_1 d\tau \cong \sum_j \sum_\alpha e^{\pm i \vec{q} \cdot \vec{R}_{j\alpha}} \int \Psi_2^* \vec{\nabla} V_{j\alpha} \Psi_2 d\tau \gg \sum_j \sum_\alpha e^{\pm i \vec{q} \cdot \vec{R}_{j\alpha}} \int \Psi_1^* \vec{\nabla} V_{j\alpha} \Psi_2 d\tau . \qquad (A7)$$

The condition approximately equal to Eq. (A7) is realized under the conditions of $E_F \gg \frac{1}{2}\gamma_1$. Equation (A7) corresponds to $D_{11} \cong D_{22} \gg D_{12} = D_{21}$ in Eq. (14).

*Permanent address: Central Research Laboratory, Matsushita Electric Industrial Co., Ltd. Moriguchi, Osaka 570, Japan.

[1]M. S. Dresselhaus and G. Dresselhaus, Adv. Phys. 30, 139 (1981).

[2]B. Poulaert, J. Heremans, J.-P. Issi, I. Zabala, H. Mazurek, and M. S. Dresselhaus, Extended Abstracts, Biennial Conference on Carbon, Philadelphia, 1981 (in press), p. 92.

[3]J.-P. Issi, J. Boxus, B. Poulaert, H. Mazurek, and M. S. Dresselhaus, J. Phys. C 14, L307 (1980).

[4]J. Heremans, J.-P. Issi, I. Zabala-Martinez, M. Shayegan, and M. S. Dresselhaus, Phys. Lett. 84A, 387 (1981).

[5]J.-P. Issi, B. Poulaert, J. Heremans, and M. S. Dresselhaus, Solid State Commun. (in press).

[6]M. Elzinga, D. T. Morelli, and C. Uher, Phys. Rev. B 26, 3312 (1982).

[7]T. Tsuzuku and K. Sugihara, Chemistry and Physics of Carbon, edited by P. L. Walker and P. A. Thrower (Dekker, New York, 1975), Vol. 12, p. 109.

[8]K. Sugihara, J. Phys. Soc. Jpn. 29, 1465 (1970).

[9]K. Sugihara, T. Takezawa, T. Tsuzuku, Y. Hishiyama, and A. Ono, J. Phys. Chem. Solids 33, 1475 (1972).

[10]J. P. Jay-Gerin and R. Maynard, J. Low Temp. Phys. 3, 337 (1970).

[11]J. Blinowski, N. H. Hau, C. Rigaux, J. P. Vieren, R. LeToullec, G. Furdin, A. Herold, and J. Melin, J. Phys. (Paris) 41, 47 (1980).

[12]S. Y. Leung and G. Dresselhaus, Phys. Rev. B 24, 3490 (1981).

[13]J. Giergiel, P. C. Eklund, R. Al-Jishi, and G. Dresselhaus (unpublished); R. Al-Jishi, Ph.D. thesis, Massachusetts Institute of Technology, 1982 (unpublished).

[14]K. Sugihara and H. Sato, J. Phys. Soc. Jpn. 18, 332 (1963); S. Ono and K. Sugihara, ibid. 21, 861 (1966); J. W. McClure and L. B. Smith, Proceedings of the 5th Carbon Conference, Pennsylvania, 1962, edited by S. Mrozowski (Pergamon, New York, 1963), Vol. II, p. 3.

[15]L. E. Gurevich and I. Ya. Korenblit, Fiz. Tverd. Tela (Len-

ingrad) $\underline{9}$, 1195 (1967) [Sov. Phys.—Solid State $\underline{9}$, 932 (1967)].

[16]D. E. Soule, Phys. Rev. $\underline{112}$, 698 (1958); $\underline{112}$, 708 (1958).

[17]K. Sugihara, K. Kawamura, and T. Tsuzuku, J. Phys. Soc. Jpn. $\underline{47}$, 1210 (1979).

[18]L. W. Kreps and J. A. Woollam, Carbon $\underline{15}$, 403 (1977).

[19]B. Dreyfus and R. Maynard, J. Phys. (Paris) $\underline{28}$, 955 (1967).

[20]B. T. Kelly, Carbon $\underline{5}$, 247 (1967).

[21]J.-P. Issi, J. Heremans, and M. S. Dresselhaus, Phys. Rev. B $\underline{27}$, 1333 (1983).